Craniospinal proton therapy

Supine craniospinal irradiation in pediatric patients by proton pencil beam scanning

Paolo Farace [a,*], Nicola Bizzocchi [a], Roberto Righetto [a], Francesco Fellin [a], Francesco Fracchiolla [a], Stefano Lorentini [a], Lamberto Widesott [a], Carlo Algranati [a], Barbara Rombi [a], Sabina Vennarini [a], Maurizio Amichetti [a], Marco Schwarz [a,b]

[a] Proton Therapy Center, Hospital of Trento, Azienda Provinciale per I Servizi Sanitari (APSS), Italy; and [b] Trento Institute for Fundamental Physics and Applications (TIFPA), National Institute of Nuclear Physics (INFN), Trento, Italy

ABSTRACT

Background and purpose: Proton therapy is the emerging treatment modality for craniospinal irradiation (CSI) in pediatric patients. Herein, special methods adopted for CSI at proton Therapy Center of Trento by pencil beam scanning (PBS) are comprehensively described.
Materials and methods: Twelve pediatric patients were treated by proton PBS using two/three isocenters. Special methods refer to: (i) patient positioning in supine position on immobilization devices crossed by the beams; (ii) planning field-junctions via the ancillary-beam technique; (iii) achieving lens-sparing by three-beams whole-brain-irradiation; (iv) applying a movable-snout and beam-splitting technique to reduce the lateral penumbra. Patient-specific quality assurance (QA) program was performed using two-dimensional ion chamber array and γ-analysis. Daily kilovoltage alignment was performed.
Results: PBS allowed to obtain optimal target coverage (mean D98% > 98%) with reduced dose to organs-at-risk. Lens sparing was obtained (mean D1 $\sim$ 730 cGyE). Reducing lateral penumbra decreased the dose to the kidneys (mean Dmean < 600 cGyE). After kilovoltage alignment, potential dose deviations in the upper and lower junctions were small (average 0.8% and 1.2% respectively). Due to imperfect modeling of range shifter, QA showed better agreements between measurements and calculations at depths >4 cm (mean γ > 95%) than at depths < 4 cm.
Conclusions: The reported methods allowed to effectively perform proton PBS CSI.

© 2017 Elsevier B.V. All rights reserved. Radiotherapy and Oncology 123 (2017) 112–118

Craniospinal radiotherapy is an irradiation technique frequently used in the treatment of malignant childhood tumors. Late toxicity is a major problem in long-term survivors and significantly affects their quality of life.

There is an increasing evidence that proton therapy allows performing craniospinal irradiation (CSI) with equivalent disease control with respect to conventional photon radiation therapy [1], but with less toxicity [2]. Particularly, in pediatric medulloblastoma the compelling dosimetric data and clinical results recently presented by Yock et al. [3], suggested that proton therapy has to be considered the preferred irradiation modality for CSI.

In this perspective, the optimal methods to deliver proton CSI in pediatric patients need to be deeply investigated. Specific technical problems include: field junction [4–6], restriction in beam entrance due to the presence of immobilization devices [7], whole brain irradiation [8–10] including coverage of the cribriform plate, positioning of the patient in supine position [11] to improve compliance and facilitate anesthesia, optimization of the spinal fields and, finally, the use of active pencil beam scanning (PBS) instead of passive scattering [12].

Even though active PBS did not always provide better plan quality [13], it can significantly reduce the risk of second cancer with respect to passive scattering [14]. Whereas in pediatric CSI both active and passive scanning modes provided a marked decreased risk with respect to photon therapy [15,16], PBS can markedly limit undesired neutron production, which might be highly effective in inducing second cancers [17].

Nowadays there are few published studies that comprehensively describe the clinically applied treatment techniques for proton CSI: a standard method was proposed with passive scattering [18] and, to our knowledge, there is only one comprehensive study with PBS [5].

The present study describes the methods developed and adopted at our department to plan and deliver CSI by proton PBS

* Corresponding author at: Proton therapy Unit – Hospital of Trento, Via del Desert 14, 38122 Trento, Italy.
E-mail address: paolofarace@gmail.com (P. Farace).

in supine position, including details and results of patient-specific quality assurance (QA) and image guided (IGRT) procedures.

Materials and methods

Immobilization devices

To satisfy the needs of both accurate patient positioning and the use of posterior beams, an insert (kVue Standard Insert – Qfix Systems, Avondale, PA, USA) and an overlay (Type-S Overlay Proton – CIVCO Medical Solutions, Kalona, IA, USA) were utilized. A combination of the two couches, one over the other, was necessary as the used head-and-neck thermoplastic mask (MDA Proton Type S-Mask – CIVCO Medical Solutions, Kalona, IA, USA) had to be fixed to the overlay. The insert was modified, smoothing an undesired protrusion on the posterior side. A fully customizable headrest (Moldcare – Qfix Systems, Avondale, PA, USA) was chosen to be crossed by the beams, due to its low density and its moldable form, which can be smoothed in the direction perpendicular to the beam.

As recommended in the report of the AAPM Task Group 176 [19], the treatment planning system (TPS) was used to calculate the water equivalent thickness (WET) of the immobilization device, comparing TPS-calculated WET with measurements, to ensure that the devices were properly modeled. Herein, masks, couches and headrest were considered as portions of the patient and included in the external contour for dose calculation [20].

Treatment planning

From October 2015 to September 2016 twelve CSI pediatric patients (mean age 7.5 years, range 5–17 years) were treated by a Proteus®Plus proton therapy system (Ion Beam Application SA – IBA – Louvain-La-Neuve, Belgium), equipped with PBS technology (minimum/maximum energy 70/226 MeV; range shifter WET 4.1 cm; spot size in air without range shifter: ~6.7 mm at 70 MeV, ~4.9 mm at 100 MeV, ~2.7 mm at 226 MeV; spot size in air with range shifter at 100 MeV: ~6.5 mm with maximal snout extension, ~11.1 mm with snout retracted). Treatment plans were generated by XIO (IMPAC Medical Systems, Stockholm, Sweden) for the first four patients and then, due to a change of the TPS, by RayStation (RaySearch Laboratories, Stockholm, Sweden) for the remaining eight patients.

All patients had a CT scan in supine position with 3 mm slices through the entire cranium and spinal region including all organs and structures of the pelvis. For skeletally immature children, the clinical target volume (CTV) included whole brain with the cribriform plate, optic nerves and in the spine, the subarachnoid space, whole vertebral body and spinal nerve roots. For skeletally mature patients, the CTV included only the subarachnoid space and spinal nerve roots. The inferior border of CTV was identified at the end of dural sac (generally to S3 vertebral level) by high resolution pre-irradiation sagittal spine MRI. A PTV was created as a 4-mm uniform expansion of the CTV. In addition, the following organs at risk (OARs) were outlined: lens, cochleae, eyes, thyroid gland, larynx, esophagus, heart, lungs, bowel, spleen, liver and kidneys. For standard risk patients, the prescribed dose was 23.4 GyE in 13 fractions. For high-risk patients, CSI dose was 36 GyE in 20 fractions.

Two or three isocenters were used, depending on the PTV length. All isocenters were positioned at midline and were 10 cm from the couch antero-posteriorly. Cranio-caudally, the cranial isocenter was positioned at the level of the foramen magnum, and the isocenter(s) of the spinal fields were positioned so that the corresponding beam sizes were symmetric.

The PTV was subdivided into three to five planning optimization volumes (POV): one brain POV, one upper junction POV, and one or two spinal POV plus an additional lower junction POV depending on the number of isocenters. The limits of the upper junction were defined by the cranial isocenter and by the level of the shoulder, i.e. the maximum feasible length considering that the cranial and spinal PTV were treated by different beam arrangements. When it was present, the lower junction either had the same length as the upper junction or it was longer, as there were no anatomical but only technical restrictions, due to the maximum available field size (40 cm).

Fields geometry included two lateral plus a posterior beam for brain irradiation and a posterior beam at each isocenter to treat the spine. Single-field optimization (SFO) was always applied to ensure robust target coverage [21], as it is generally agreed that SFO-IMPT is more robust than multi-field optimization (MFO-IMPT) [22,23].

To plan the field junction, a recently developed gradient-optimized method using ancillary beams [6] was implemented on both TPSs. The ancillary beam consisted of high energy layers of pencil beams at the maximum energy (226 MeV) with variable monitor units along the cranio-caudal direction to produce a linear dose gradient in the overlapping region (i.e. in the junction POVs) between adjacent treatment beams. The ancillary beam was used in the background during the inverse planning optimization of the upper spinal beam and then deleted. The resulting spinal beam produced a slow, linear and complementary dose gradient at its edges, and it was used in background during the inverse planning of the other beams.

All beams were planned taking advantage of a new movable 'snout' and a 'beam splitting' technique to reduce the lateral penumbra. Thanks to the first feature, the range shifter was moved as close as possible to the patient surface by a movable snout system. The latter consisted of splitting each beam in two components, i.e. if a beam required a range shifter, two sub-beams were created. The first sub-beam has a range shifter and includes only the energy layers needed to irradiate the target at depths lower then 4 cm WET. The second sub-beam has all remaining layers, which do not require the range shifter. This allows to use the range shifter only when it is actually needed and to obtain both better lateral penumbra and better agreement between measurements and calculations. The two sub-beams were then optimized simultaneously, obtaining in such a way an SFO dose distribution.

Whole brain irradiation was performed by a lens-sparing three-beam technique [24]. Such three-beam arrangement for brain irradiation includes two lateral opposed beams (gantry angle 90° and 270°), with couch angle ±15° to minimize the overlap between the cribriform plate and the lens, and an additional 180° posterior beam. During SFO of the three equally-weighted beams, coverage of the cribriform plate is assumed as the primary goal and lens sparing as a secondary objective.

In an exemplary case this new technique was compared with a SFO two-beams oblique-posterior technique and a SFO two-beams opposed-lateral technique.

On the same case, to evaluate the robustness of the three-beam technique, a worse case robust evaluation was performed (3.5% range uncertainty and 2 mm setup errors) to assess the coverage of the cribriform plate and the dose to the lens. The simulated setup errors are still conservative considering the daily imaging protocol used for patient positioning.

Patient-specific QA

Our current patient-specific QA program consisted of two parts: (i) an end-to-end test performed at the planned gantry angles with an ionization chamber (data not reported) and (ii) a dose comparison on two-dimensional planar dose distributions. The second set of measurements, consisting of two (typically for the spinal beams) or three (for the cranial beams) depth measurements for each field,

were delivered with the gantry at 0° and measured using an ion chamber array with a plastic water phantom. The measured dose planes were compared with the dose planes calculated by TPS, and evaluated using the gamma index with dose tolerance 3% of beam prescription dose, distance to agreement 3 mm and threshold 5%.

IGRT and treatment workflow

Before each treatment session, patients were aligned by kilovoltage orthogonal imaging. All three isocenters (cranial, spinal I and spinal II) were verified according to the following workflow:

– Laser pre-alignment of immobilized patient on the cranial isocenter; kilo-voltage alignment and application of the resulting correction vector. The final position is memorized in the record-and-verify (r&v) system.
– Translation to isocenter spinal II. Kilo-voltage alignment was verified. When cranio-caudal correction greater than 3 mm or rotations were required, the patient was repositioned. If it was not necessary, the correction vector was separately registered, but not yet applied.
– Translation to isocenter spinal I; kilo-voltage alignment and application of the resulting correction vector. Irradiation of the upper spinal beam.
– Translation to isocenter spinal II and application of the correction vector previously registered. Verification by Kilo-voltage imaging. Irradiation of the lower spinal beam.
– Translation to the corrected cranial isocenter previously memorized in the r&v system and irradiation of the cranial beams.

When only two isocenters were planned, the above workflow was simplified accordingly.

Only translation corrections were allowed in the cranial isocenter and only cranio-caudal and right-left translation were allowed in the spinal isocenters to minimize beam overlapping in the field junctions.

Results

Treatment planning

With the exception of patient #4 and #5, all patients were treated with three isocenters.

In Fig. 1, the average dose parameters (Dmean and D1) to target volumes and organs at risk were reported. For consistency of presentation, results for patient #9 and #10, with a prescription of 23.4 GyE, were converted to a 36 GyE prescription. PBS allowed to obtain optimal target coverage, with average D98% > 98% of the prescription dose in all the POVs, and OAR sparing.

The dose to OARs in the thorax and abdomen of the single skeletally mature patient (#3) were obviously smaller than in all other patients, due to a different CTV protrusion, and therefore they were not computed in the analysis shown in Fig. 1. In this patient, the corresponding dose parameters were smaller than 1 GyE, with only D1 to the lungs greater than 10 GyE.

The ancillary-beam junction technique (Fig. 2), allowed to reliably apply the gradient method. It was easily implemented in the first TPS, and in the second TPS a suitable script was written for its implementation. With both TPSs, its routine usage during treatment planning required a negligible additional time (around 2 min). The parameter describing the dose delivered on the junction region (Fig. 1) showed uniform dose on both junctions.

An example of the kidney-sparing technique is reported in Fig. 3. The splitting technique allowed to halve the Dmean to the kidneys. The snout extension allowed to further slightly improve kidney sparing. Accordingly, in patient #1 (planned with no splitting and no snout extension) and patient #2 (planned with snout extension but no splitting) the dose to the kidney was greater than in the other successive patients. Considering patients #4–12, the mean Dmean to the kidneys was less than 6 GyE.
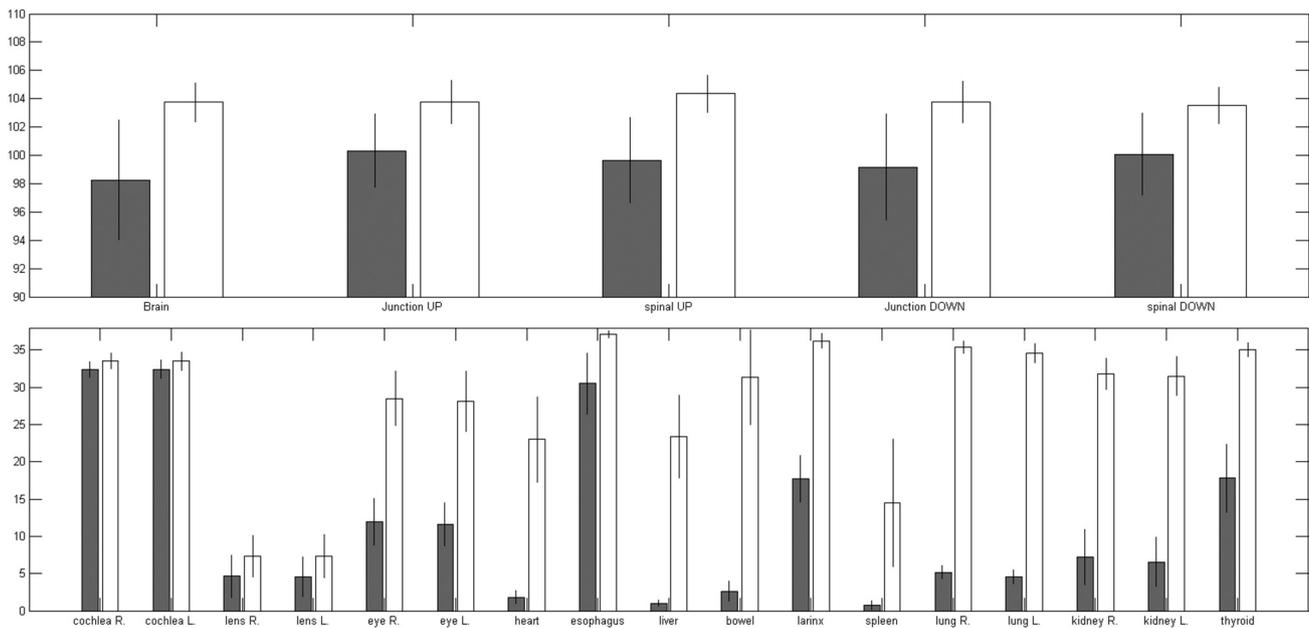
Fig. 1. Plan evaluation parameters. Dosimetric parameters on POVs (planning optimization volumes, top) and on OARs (organs at risk, bottom) obtained averaging on twelve pediatric patients. The vertical lines represent standard deviations. Dmean (gray bar) and D1 (white bar) are shown. In the ordinate, POVs dose are reported as a% of the prescription dose (36 GyE), and OARs dose are reported in GyE. For consistency of presentation, results for patient #9 and #10, with a prescription of 23.4 GyE, were converted to 36 GyE prescription. The OARs in the thorax and abdomen of the single skeletally mature patient (#3) were not included in the computation, as the corresponding dose parameters were markedly smaller.
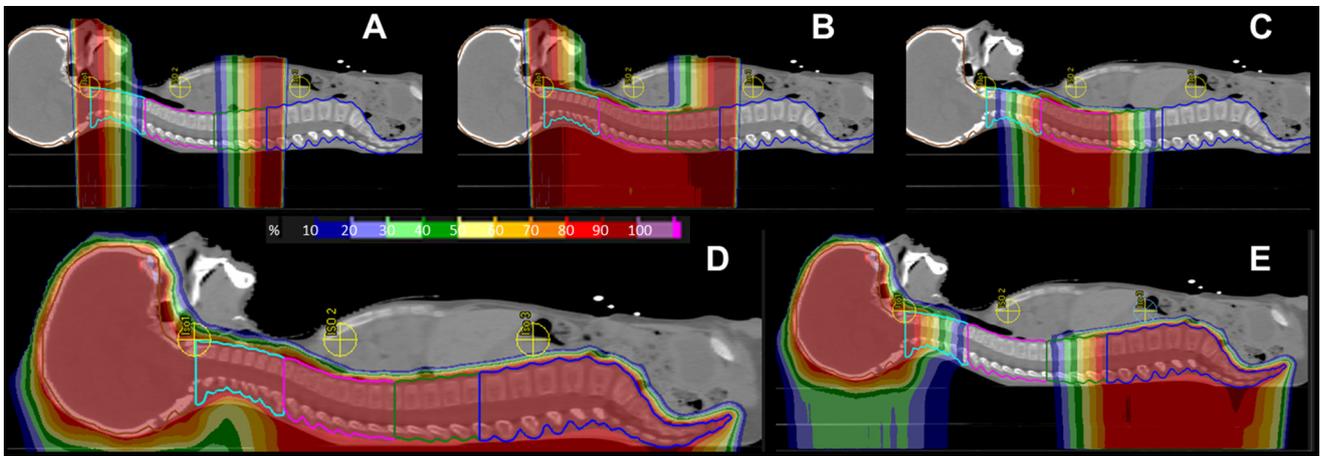
Fig. 2. Planning field-junction by the ancillary beam technique. The ancillary beams (A) are used to inversely plan the upper spinal beam (B) and then deleted. The resulting upper spinal beam (C) is switched on during the optimization of the cranial and lower spinal beams to obtain the final dose distribution (D). The dose distribution of the resulting cranial and lower spinal beams is shown in (E). The positions of the three isocenters are also shown. The dose scale refers to all the image and it is reported in% of the prescription dose (36 GyE).
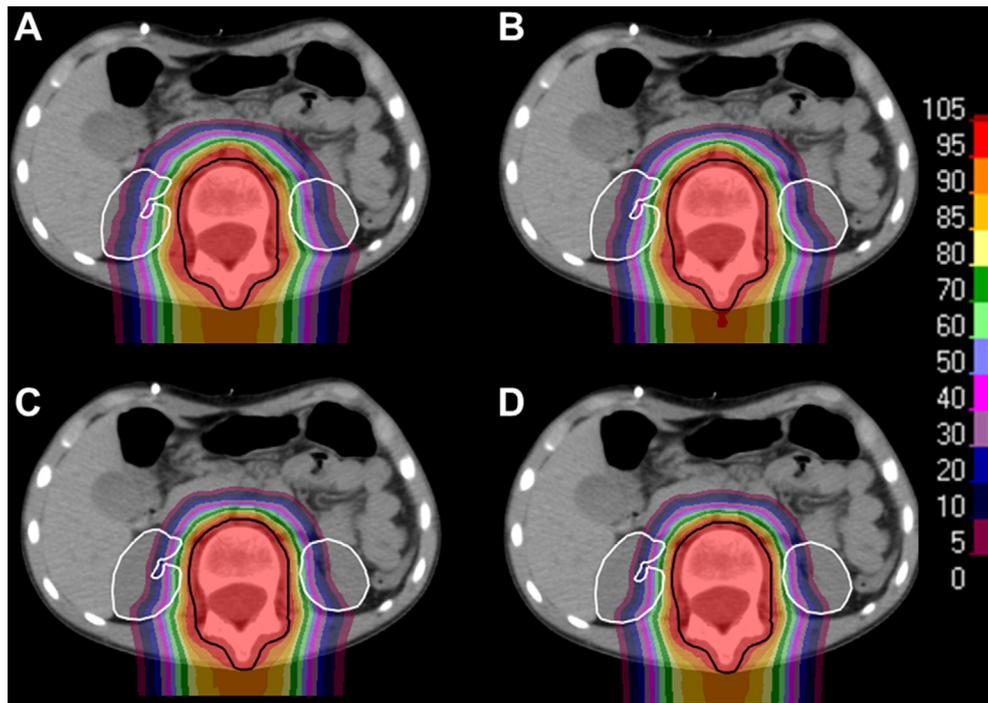
Fig. 3. Kidney sparing by splitting technique and snout extension. (A) Single posterior beam technique with no split and no snout extension (air gap = 21 cm) delivering a kidney mean dose = 13.1 Gy. (B) Single posterior beam technique with no split but snout extension (air gap = 12 cm) delivering a kidney mean dose = 12.0 Gy. (C). Two posterior beams splitting technique, without snout extension (air gap = 21 cm), delivering a kidney mean dose = 8.6 Gy. (D) Two posterior beams splitting technique, with snout extension (air gap = 12 cm) of the beam with the range shifter, delivering a kidney mean dose = 8.5 Gy. The dose scale refers to all the images and it is reported in% of the prescription dose (36 GyE).

An example of the lens-sparing technique is shown in Supplementary Materials (Fig. S1), where it is also compared with two more conventional approaches: two angled (±20°) oblique-posterior beams and two opposed-lateral beams. Adequate target coverage is obtained by all beam arrangements, but the new lens-sparing technique allowed to markedly decrease the dose to the lenses. Comparing the three different techniques (three-beam, two oblique-posterior and two opposed-lateral) in this exemplary case, the corresponding D1 were 5.8 GyE, 15.7 GyE and 17.6 GyE to the right lens and 6.0 GyE, 15.7 GyE and 17.5 GyE to the left lens, respectively. Robustness evaluation performed on the same case (see Fig. S2 in Supplementary Materials) showed negligible variation in the coverage of the cribriform plate (D95% > 36 GyE; D98% > 35.8 GyE). The greater dose to the lenses in the worst case (max D1 ∼ 9 GyE) resulted still smaller than the dose, reported above, obtained with the other beam arrangements in the nominal scenario.

The data reported in Fig. 1 confirmed a good lens-sparing in the patient group treated by the new three-beams technique, with mean D1 around 7.3 GyE.

Table 1
Image-guided correction vectors and corresponding potential dose deviation.

#	Spinal isocenter I (cranial)				Spinal isocenter II (caudal)			
	X (cm)	Y (cm)	Junction length (cm)	% dose deviation[*]	X (cm)	Y (cm)	Junction length (cm)	% dose deviation[*]
1	−0.07 ± 0.20	0.21 ± 0.08	6.00	3.5	0.03 ± 0.24	0.01 ± 0.11	6.90	0.1
2	−0.18 ± 0.19	−0.03 ± 0.07	8.70	−0.4	0.01 ± 0.28	−0.01 ± 0.13	8.70	−0.1
3	−0.11 ± 0.16	0.08 ± 0.07	9.00	0.9	0.04 ± 0.22	0.13 ± 0.11	8.70	1.4
4	−0.01 ± 0.10	−0.07 ± 0.07	4.20	-1.7	N.A[**]	N.A[**]	N.A[**]	N.A[**]
5	−0.06 ± 0.17	0.03 ± 0.08	5.10	0.6	N.A[**]	N.A[**]	N.A[**]	N.A[**]
6	0.00 ± 0.09	0.02 ± 0.06	8.10	0.3	−0.05 ± 0.13	−0.01 ± 0.08	8.10	−0.1
7	0.03 ± 0.20	0.04 ± 0.08	8.00	0.5	−0.08 ± 0.24	0.17 ± 0.14	8.00	2.1
8	−0.04 ± 0.07	0.02 ± 0.04	7.50	0.3	−0.04 ± 0.16	0.16 ± 0.11	7.80	2.0
9	0.00 ± 0.07	0.02 ± 0.07	4.80	0.5	0.13 ± 0.18	0.01 ± 0.09	7.80	0.2
10	−0.04 ± 0.07	−0.03 ± 0.07	6.00	−0.5	0.00 ± 0.14	0.08 ± 0.13	6.00	1.3
11	0.04 ± 0.09	0.01 ± 0.04	7.00	0.2	−0.02 ± 0.20	0.27 ± 0.04	7.00	3.8
12	0.19 ± 0.14	0.02 ± 0.08	8.00	0.3	−0.19 ± 0.20	0.07 ± 0.14	8.00	0.8

Correction along the right-left (X) and the cranio-caudal (Y) direction are reported as mean ± standard deviation.
 [*] Dose deviation in the field junction were calculated according to [5,6]: % dose deviation = mean (Y)/junction lengths.
 [**] Patients #4 and #5 where treated with only two isocenters.

Patient-specific QA

The gamma passing percentages for each patient at the different depth measurements are reported as Supplementary Materials (Table S1). In general, a better agreement was observed in the deeper measurements (>4 cm) than at shallow depths (<4 cm). Almost all beams were planned by the splitting technique, so that only the measurement at depth < 4 cm involved beams with range shifter. A slight improvement can be seen for patients (#5–12) planned with the new TPS with respect to patients (#1–4) planned with the older one.

IGRT and treatment workflow

The resulting correction vectors for the spinal isocenters are reported in Table 1. Only cranio-caudal (Y) and right-left (X) translation were allowed. The minimum upper junction length was around 4 cm, due to anatomical limitation. Longer junctions were defined in the other cases. The potential dose deviations in the junctions POVs can be estimated from the average deviations along the cranio-caudal direction, showing that in only two over ten patients (#1 and #4) the dose deviation was around 2% or greater in the upper junction, and in three over eight (#7, #8 and #11) in the lower junction. In the other cases the potential dose deviations were negligible. The maximum dose deviation was 3.5% in the upper junction and 3.8% in the lower junction. Averaging on the twelve patients, the potential absolute dose deviance were 0.8% and 1.2% on the two junctions, respectively.

On average, the total in-room time was 80 min under anesthesia and 67 min without anesthesia, during which the mean time for irradiation was around 32 min.

Discussion

In this study a method to deliver PBS CSI in supine position is comprehensively described.

It is acknowledged that the supine position is better tolerated and more stable than the prone position, allowing also anesthesiologist direct access to the patient's oral cavity and airways. However, the supine position presents additional technical difficulties with respect to the prone position, due to the presence of the couch and immobilization devices along the beam path, which might affect proton range. According to recent guidelines [19], the TPS should be used to calculate the WET of the immobilization device, comparing TPS calculated WET with measurements to ensure that the devices were properly modeled. Such systematic acceptance

tests were performed [20] on the used commercially available devices. Moreover, only lateral and posterior (180°) beams were used. Particularly, in the new three-beam arrangement for whole brain irradiation it was not necessary to provide clearance to avoid passage through the couch as in other methods using oblique-posterior beams [7].

CSI field–junctions planning techniques have often been investigated over the course of the years, evolving from the moving junction techniques, often referred to as 'field feathering', to the method exploiting the potential of dose modulation and inverse planning. It has been recently shown that the field-junction most robust to setup errors is obtained by the so-called gradient-optimized methods, i.e. by producing a slow, linear and complementary dose gradient at the beam edges in the overlapping region between adjacent beams [25]. These methods showed a reduced sensitivity to longitudinal setup errors compared to the conventional feathering methods. A gradient-optimized method has been recently implemented in PBS, by generating multiple optimization volumes to drive the optimization [5]. However, as reported by the same authors, this method required a significant amount of time to delineate the optimization structures for optimizing the dose in the junction area. In our study, it was successfully demonstrated, in two different commercially available TPS, the feasibility of the alternative ancillary beam technique [6]. Once it has been implemented, this technique did not require significant amount of time for routine application and avoided cumbersome contouring and planning procedures. Set-up errors measured during the IGRT procedure showed that a maximum potential dose deviance of 3.5% was caused in the upper junction and 3.8% in the lower junction. These potential overdosages had to be taken into account to plan the boost phase. The estimated dose deviance was within 2% in the other cases.

Regarding IGRT procedures and treatment workflow, both spinal fields were treated immediately after the application of the displacement correction vectors, so that intra-fractional movements are minimized. The correction vector of the cranial isocenter was calculated at the beginning of the IGRT procedure, and the cranial beams were delivered at the end of the irradiation procedure. This long time increased the possibility of intra-fractional movements, which were minimal due to the immobilization mask (as we occasionally re-verified in some patients – data not shown) and, in most of the patients, due to treatment under anesthesia. The treatment time was slightly longer than that reported by another PBS study [5]. The irradiation time was around 32 min compared to less than 20. It included not only beam-on time but also the time to move the couches and the gantry at different

angles. Nevertheless, the setup mean time seems quite long, with a total in-room time of 67 min compared to 45 min. It could be partially due to our complex IGRT workflow, but it could be presumably reduced in the future when all the operators are fully confident with the procedure.

In PBS the quality of dose distributions strongly depends on the spot size [26]. As a consequence, the use of range shifter with large air gaps negatively affects plan quality, due to the unavoidable increase in spot size. To reduce these effects, all beams were planned by a new splitting technique, so that the range shifter was used only in the layers where it was really necessary. A clear effect of the reduced spot size was observed in the dose delivered to the kidney by the posterior spinal beams. Moreover, a movable snout allowed to position the range shifter as close as possible to the skin surface, further reducing the resulting spot size in the patient. Apart from the splitting technique, to treat the spine we used conventional posterior beams, like in [5].

The results of patients-specific QA were slightly worse compared to those reported by other authors [27], where the gamma passing rate was 94.8% ± 0.6% for fields with range shifter and 99.0% ± 0.6% for those without. Accordingly, in the present study patient-specific QA evidenced a better general agreement in the deeper measurements (>4 cm) than in the more superficial ones (<4 cm). This difference is likely due to the less accurate modeling of the layers with range shifter [28], as it is not accurately modeled as a scattering source in the TPS. The extensive use of the splitting technique minimized the number of layers delivered with the range shifter, thus potentially improving the agreement between measurements and predictions. However, the TPS systematically underestimated (around 2–3%) the delivered dose, excluding any risk of target under-dosage. When performing the gamma analysis with dose tolerance 5% (instead of 3%) of beam prescription dose, the passing rates were above 95% at all depths (data not shown). Furthermore, the agreement along the dose gradient profile in the junction area was very good (data not shown), also supported by tests performed on spot position (difference between nominal and measured position <1 ± 0.5 mm) at field edges (around 17.5 cm from isocenter).

Finally, one of the main problems in CSI is the sparing of the lens to avoid cataract formation without under-dosage to the cribriform plate, which may lead to treatment failure. This difficulty is more pronounced in younger patients because of anatomic effects of sinus development [10]. A three-beam technique was utilized, as it was superior [24] to other techniques, such as two lateral beams [5,8] or two oblique-posterior beams [10,18]. In the three-beam arrangement, a posterior beam is included. With this beam the eyes and the cribriform plate are located at the distal end, where potential range uncertainty may cause dose uncertainty. However, as the three beams were equally weighted, this beam accounted for only one third of the dose and thus any potential dose uncertainty was proportionally reduced, as confirmed by robustness analysis.

In conclusion, this study described technical methods that allowed to efficiently plan and to effectively deliver high quality CSI by PBS in pediatric patients. These methods might be adopted in other facilities equipped with proton PBS technology.

Conflict of interest statement

Authors have no conflict of interest to declare.

Appendix A. Supplementary data

Supplementary data associated with this article can be found, in the online version, at http://dx.doi.org/10.1016/j.radonc.2017.02.008.

References

[1] Eaton BR, Esiashvili N, Kim S, Weyman EA, Thornton LT, Mazewski C, et al. Clinical outcomes among children with standard-risk medulloblastoma treated with proton and photon radiation therapy: a comparison of disease control and overall survival. Int J Radiat Oncol Biol Phys 2016;94(1):133–8.

[2] Brown AP, Barney CL, Grosshans DR, McAleer MF, de Groot JF, Puduvalli VK, et al. Proton beam craniospinal irradiation reduces acute toxicity for adults with medulloblastoma. Int J Radiat Oncol Biol Phys 2013;86(2):277–84.

[3] Yock TI, Yeap BY, Ebb DH, Weyman E, Eaton BR, Sherry NA, et al. Long-term toxic effects of proton radiotherapy for paediatric medulloblastoma: a phase 2 single-arm study. Lancet Oncol 2016;17(3):287–98.

[4] Stoker JB, Grant J, Zhu XR, Pidikiti R, Mahajan A, Grosshans DR. Intensity modulated proton therapy for craniospinal irradiation: organ-at-risk exposure and a low-gradient junctioning technique. Int J Radiat Oncol Biol Phys 2014;90(3):637–44.

[5] Lin H, Ding X, Kirk M, Liu H, Zhai H, Hill-Kayser CE, et al. Supine craniospinal irradiation using a proton pencil beam scanning technique without match line changes for field junctions. Int J Radiat Oncol Biol Phys 2014;90(1):71–8.

[6] Farace P, Vinante L, Ravanelli D, Bizzocchi N, Vennarini S. Planning field-junction in proton cranio-spinal irradiation – the ancillary-beam technique. Acta Oncol 2015;54(7):1075–8.

[7] Barney CL, Brown AP, Grosshans DR, McAleer MF, de Groot JF, Puduvalli V, et al. Technique, outcomes, and acute toxicities in adults treated with proton beam craniospinal irradiation. Neuro Oncol 2014;16(2):303–9.

[8] Jin H, Hsi W, Yeung D, Li Z, Mendenhall NP, Marcus Jr RB. Dosimetric characterization of whole brain radiotherapy of pediatric patients using modulated proton beams. J Appl Clin Med Phys 2011;12(2):3308.

[9] Dinh J, Stoker J, Georges RH, Sahoo N, Zhu XR, Rath S, et al. Comparison of proton therapy techniques for treatment of the whole brain as a component of craniospinal radiation. Radiat Oncol 2013;17(8):289.

[10] Cochran DM, Yock TI, Adams JA, Tarbell NJ. Radiation dose to the lens during craniospinal irradiation-an improvement in proton radiotherapy technique. Int J Radiat Oncol Biol Phys 2008;70(5):1336–42.

[11] Buchsbaum JC, Besemer A, Simmons J, Hoene T, Simoneaux V, Sandefur A, et al. Supine proton beam craniospinal radiotherapy using a novel tabletop adapter. Med Dosim 2013;38:70–6.

[12] Timmermann B, Lomax AJ, Nobile L, Grotzer MA, Weiss M, Kortmann RD, et al. Novel technique of craniospinal axis proton therapy with the spot-scanning system: avoidance of patching multiple fields and optimized ventral dose distribution. Strahlenther Onkol 2007;183(12):685–8.

[13] Moteabbed M, Yock TI, Depauw N, Madden TM, Kooy HM, Paganetti H. Impact of spot size and beam-shaping devices on the treatment plan quality for pencil beam scanning proton therapy. Int J Radiat Oncol Biol Phys 2016;95(1):190–8.

[14] Geng C, Moteabbed M, Xie Y, Schuemann J, Yock T, Paganetti H. Assessing the radiation-induced second cancer risk in proton therapy for pediatric brain tumors: the impact of employing a patient-specific aperture in pencil beam scanning. Phys Med Biol 2016;61(1):12–22.

[15] Newhauser WD, Fontenot JD, Mahajan A, Kornguth D, Stovall M, Zheng Y, et al. The risk of developing a second cancer after receiving craniospinal proton irradiation. Phys Med Biol 2009;54(8):2277–91.

[16] Yoon M, Shin DH, Kim J, Kim JW, Kim DW, Park SY, et al. Craniospinal irradiation techniques: a dosimetric comparison of proton beams with standard and advanced photon radiotherapy. Int J Radiat Oncol Biol Phys 2011;81(3):637–46.

[17] Taddei PJ, Mahajan A, Mirkovic D, Zhang R, Giebeler A, Kornguth D, et al. Predicted risks of second malignant neoplasm incidence and mortality due to secondary neutrons in a girl and boy receiving proton craniospinal irradiation. Phys Med Biol 2010;55(23):7067–80.

[18] Giebeler A, Newhauser WD, Amos RA, Mahajan A, Homann K, Howell RM. Standardized treatment planning methodology for passively scattered proton craniospinal irradiation. Radiat Oncol 2013;3(8):32.

[19] Olch AJ, Gerig L, Li H, Mihaylov I, Morgan A. Dosimetric effects caused by couch tops and immobilization devices: report of AAPM Task Group 176. Med Phys 2014;41(6):061501.

[20] Fellin F, Righetto R, Fava G, Trevisan D, Amelio D, Farace P, et al. Water equivalent thickness of immobilization devices in proton therapy planning – Modelling at treatment planning and validation by measurements with a multi-layer ionization chamber. Phys Med 2017. http://dx.doi.org/10.1016/j.ejmp.2017.02.010.

[21] Quan EM, Liu W, Wu R, Li Y, Frank SJ, Zhang X, et al. Preliminary evaluation of multifield and single-field optimization for the treatment planning of spot-scanning proton therapy of head and neck cancer. Med Phys 2013;40(8):081709.

[22] Albertini F, Hug EB, Lomax AJ. Is it necessary to plan with safety margins for actively scanned proton therapy? Phys Med Biol 2011;56(14):4399–413.

[23] Farace P, Righetto R, Cianchetti M. Single-energy intensity modulated proton therapy. Phys Med Biol 2015;60(19):N357–67.

[24] Bizzocchi N, Rombi B, Farace P, Algranati C, Righetto R, Schwarz M, et al. A planning approach for lens sparing proton craniospinal irradiation in pediatric patients. ESTRO 35. 2016 29 April–3 May; EP-1691.

[25] Hadley A, Ding GX. A single-gradient junction technique to replace multiple-junction shifts for craniospinal irradiation treatment. Med Dosim 2014;39:314–9.

[26] Widesott L, Lomax AJ, Schwarz M. Is there a single spot size and grid for intensity modulated proton therapy? Simulation of head and neck, prostate and mesothelioma cases. Med Phys 2012;39(3):1298–308.

[27] Mackin D, Zhu XR, Poenisch F, Li H, Sahoo N, Kerr M, et al. Spot-scanning proton therapy patient-specific quality assurance: results from 309 treatment plans. Int J Particle Ther 2014;1(3):711–20.

[28] Fracchiolla F, Lorentini S, Widesott L, Schwarz M. Characterization and validation of a Monte Carlo code for independent dose calculation in proton therapy treatments with pencil beam scanning. Phys Med Biol 2015;60(21):8601–19.